

Hadron Spectroscopy and Structure from AdS/CFT

Stanley J. Brodsky¹

Stanford Linear Accelerator Center
Stanford University
Stanford, California 94309

Abstract. The AdS/CFT correspondence between conformal field theory and string states in an extended space-time has provided new insights into not only hadron spectra, but also their light-front wavefunctions. We show that there is an exact correspondence between the fifth-dimensional coordinate of anti-de Sitter space z and a specific impact variable ζ which measures the separation of the constituents within the hadron in ordinary space-time. This connection allows one to predict the form of the light-front wavefunctions of mesons and baryons, the fundamental entities which encode hadron properties and scattering amplitudes. A new relativistic Schrödinger light-front equation is found which reproduces the results obtained using the fifth-dimensional theory. Since they are complete and orthonormal, the AdS/CFT model wavefunctions can be used as an initial ansatz for a variational treatment or as a basis for the diagonalization of the light-front QCD Hamiltonian. A number of applications of light-front wavefunctions are also discussed.

PACS. 12.38.Aw,12.38.-t,11.25.Hf,11.90.+t,11.55.Jy

1 Hadron Wavefunctions in QCD

One of the most important tools in atomic physics is the Schrödinger wavefunction; it provides a quantum mechanical description of the position and spin coordinates of nonrelativistic bound states at a given time t . Clearly, it is an important goal in hadron and nuclear physics to determine the wavefunctions of hadrons in terms of their fundamental quark and gluon constituents.

Guy de Téramond and I have recently shown how one can use AdS/CFT to not only obtain an accurate description of the hadron spectrum for light quarks, but also how to obtain a remarkably simple but realistic model of the valence wavefunctions of mesons, baryons, and glueballs. As I review below, the amplitude $\Phi(z)$ describing the hadronic state in the fifth dimension of Anti-de Sitter space AdS_5 can be precisely mapped to the light-front wavefunctions $\psi_{n/h}$ of hadrons in physical space-time [1], thus providing a relativistic description of hadrons in QCD at the amplitude level. The light-front wavefunctions are relativistic and frame-independent generalizations of the familiar Schrödinger wavefunctions of atomic physics, but they are determined at fixed light-cone time $\tau = t + z/c$ —the “front form” advocated by Dirac—rather than at fixed ordinary time t .

Formally, the light-front expansion is constructed by quantizing QCD at fixed light-cone time [2] $\tau = t + z/c$ and forming the invariant light-front Hamiltonian: $H_{LF}^{QCD} = P^+P^- - \mathbf{P}_\perp^2$ where $P^\pm = P^0 \pm P^z$. [3] The momentum generators P^+ and \mathbf{P}_\perp are kinematical; *i.e.*, they are independent of the interactions. The generator $P^- =$

$i\frac{d}{d\tau}$ generates light-front time translations, and the eigen-spectrum of the Lorentz scalar H_{LF}^{QCD} gives the mass spectrum of the color-singlet hadron states in QCD together with their respective light-front wavefunctions. For example, the proton state satisfies: $H_{LF}^{QCD} |\psi_p\rangle = M_p^2 |\psi_p\rangle$. Remarkably, the light-front wavefunctions are frame-independent; thus knowing the LFWFs of a hadron in its rest frame determines the wavefunctions in all other frames.

Given the light-front wavefunctions $\psi_{n/H}(x_i, \mathbf{k}_{\perp i}, \lambda_i)$, one can compute a large range of hadron observables. For example, the valence and sea quark and gluon distributions which are measured in deep inelastic lepton scattering are defined from the squares of the LFWFS summed over all Fock states n . Form factors, exclusive weak transition amplitudes [4] such as $B \rightarrow \ell\nu\pi$, and the generalized parton distributions [5] measured in deeply virtual Compton scattering are (assuming the “handbag” approximation) overlaps of the initial and final LFWFS with $n = n'$ and $n = n' + 2$. The gauge-invariant distribution amplitude $\phi_H(x_i, Q)$ defined from the integral over the transverse momenta $\mathbf{k}_{\perp i}^2 \leq Q^2$ of the valence (smallest n) Fock state provides a fundamental measure of the hadron at the amplitude level [6, 7]; they are the nonperturbative input to the factorized form of hard exclusive amplitudes and exclusive heavy hadron decays in perturbative QCD. The resulting distributions obey the DGLAP and ERBL evolution equations as a function of the maximal invariant mass, thus providing a physical factorization scheme [8]. In each case, the derived quantities satisfy the appropriate operator product expansions, sum rules, and evolution

Submitted to European Physical Journal

equations. However, at large x where the struck quark is far-off shell, DGLAP evolution is quenched [9], so that the fall-off of the DIS cross sections in Q^2 satisfies inclusive-exclusive duality at fixed W^2 .

The physics of higher Fock states such as the $|uudq\bar{Q}\rangle$ fluctuation of the proton is nontrivial, leading to asymmetric $s(x)$ and $\bar{s}(x)$ distributions, $\bar{u}(x) \neq \bar{d}(x)$, and intrinsic heavy quarks $c\bar{c}$ and $b\bar{b}$ which have their support at high momentum [10]. Color adds an extra element of complexity: for example there are five-different color singlet combinations of six 3_C quark representations which appear in the deuteron's valence wavefunction, leading to the hidden color phenomena [11].

An important example of the utility of light-front wavefunctions in hadron physics is the computation of polarization effects such as the single-spin azimuthal asymmetries in semi-inclusive deep inelastic scattering, representing the correlation of the spin of the proton target and the virtual photon to hadron production plane: $\mathbf{S}_p \cdot \mathbf{q} \times \mathbf{p}_H$. Such asymmetries are time-reversal odd, but they can arise in QCD through phase differences in different spin amplitudes. In fact, final-state interactions from gluon exchange between the outgoing quarks and the target spectator system lead to single-spin asymmetries in semi-inclusive deep inelastic lepton-proton scattering which are not power-law suppressed at large photon virtuality Q^2 at fixed x_{bj} [12] (see: Fig. 1). In contrast to the SSAs arising from transversity and the Collins fragmentation function, the fragmentation of the quark into hadrons is not necessary; one predicts a correlation with the production plane of the quark jet itself. Physically, the final-state interaction phase arises as the infrared-finite difference of QCD Coulomb phases for hadron wave functions with differing orbital angular momentum. The same proton matrix element which determines the spin-orbit correlation $\mathbf{S} \cdot \mathbf{L}$ also produces the anomalous magnetic moment of the proton, the Pauli form factor, and the generalized parton distribution E which is measured in deeply virtual Compton scattering. Thus the contribution of each quark current to the SSA is proportional to the contribution $\kappa_{q/p}$ of that quark to the proton target's anomalous magnetic moment $\kappa_p = \sum_q e_q \kappa_{q/p}$. [12, 13]. The HERMES collaboration has recently measured the SSA in pion electroproduction using transverse target polarization [14]. The Sivvers and Collins effects can be separated using planar correlations; both processes are observed to contribute, with values not in disagreement with theory expectations [14,15]. The deeply virtual Compton amplitudes can be Fourier transformed to b_\perp and $\sigma = x^- P^+ / 2$ space providing new insights into QCD distributions [16–19]. The distributions in the LF direction σ typically display diffraction patterns arising from the interference of the initial and final state LFWFs [18]. The final-state interaction mechanism provides an appealing physical explanation within QCD of single-spin asymmetries. Physically, the final-state interaction phase arises as the infrared-finite difference of QCD Coulomb phases for hadron wave functions with differing orbital angular momentum. An elegant discussion of the Sivvers effect in-

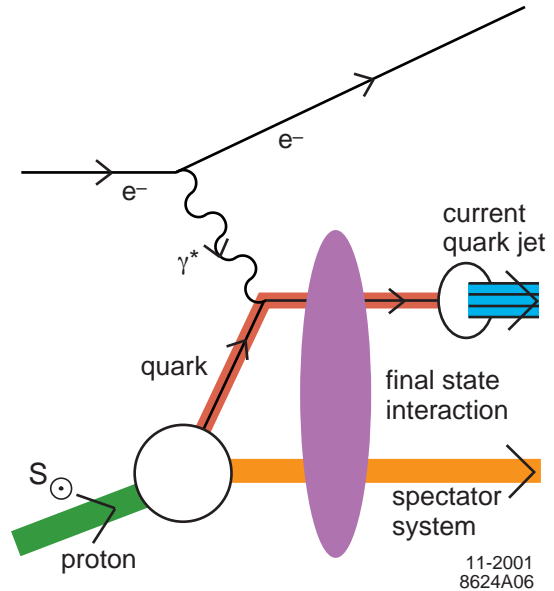


Fig. 1. A final-state interaction from gluon exchange in deep inelastic lepton scattering. The difference of the QCD Coulomb-like phases in different orbital states of the proton produces a single proton spin asymmetry.

cluding its sign has been given by Burkardt [13]. As shown by Gardner and myself [20], one can also use the Sivvers effect to study the orbital angular momentum of gluons by tagging a gluon jet in semi-inclusive DIS. In this case, the final-state interactions are enhanced by the large color charge of the gluons.

The final-state interaction effects can also be identified with the gauge link which is present in the gauge-invariant definition of parton distributions [21]. Even when the light-cone gauge is chosen, a transverse gauge link is required. Thus in any gauge the parton amplitudes need to be augmented by an additional eikonal factor incorporating the final-state interaction and its phase [22,23]. The net effect is that it is possible to define transverse momentum dependent parton distribution functions which contain the effect of the QCD final-state interactions.

A related analysis also predicts that the initial-state interactions from gluon exchange between the incoming quark and the target spectator system lead to leading-twist single-spin asymmetries in the Drell-Yan process $H_1 H_2^\dagger \rightarrow \ell^+ \ell^- X$ [24,25]. Initial-state interactions also lead to a $\cos 2\phi$ planar correlation in unpolarized Drell-Yan reactions [26].

2 Diffractive Deep Inelastic Scattering

A remarkable feature of deep inelastic lepton-proton scattering at HERA is that approximately 10% events are diffractive [27,28]: the target proton remains intact, and

there is a large rapidity gap between the proton and the other hadrons in the final state. These diffractive deep inelastic scattering (DDIS) events can be understood most simply from the perspective of the color-dipole model: the $q\bar{q}$ Fock state of the high-energy virtual photon diffractively dissociates into a diffractive dijet system. The exchange of multiple gluons between the color dipole of the $q\bar{q}$ and the quarks of the target proton neutralizes the color separation and leads to the diffractive final state. The same multiple gluon exchange also controls diffractive vector meson electroproduction at large photon virtuality [29]. This observation presents a paradox: if one chooses the conventional parton model frame where the photon light-front momentum is negative $q^+ = q^0 + q^z < 0$, the virtual photon interacts with a quark constituent with light-cone momentum fraction $x = k^+/p^+ = x_{bj}$. Furthermore, the gauge link associated with the struck quark (the Wilson line) becomes unity in light-cone gauge $A^+ = 0$. Thus the struck “current” quark apparently experiences no final-state interactions. Since the light-front wavefunctions $\psi_n(x_i, k_{\perp i})$ of a stable hadron are real, it appears impossible to generate the required imaginary phase associated with pomeron exchange, let alone large rapidity gaps.

This paradox was resolved by Paul Hoyer, Nils Marchal, Stephane Peigne, Francesco Sannino and myself [30]. Consider the case where the virtual photon interacts with a strange quark—the $s\bar{s}$ pair is assumed to be produced in the target by gluon splitting. In the case of Feynman gauge, the struck s quark continues to interact in the final state via gluon exchange as described by the Wilson line. The final-state interactions occur at a light-cone time $\Delta\tau \simeq 1/\nu$ shortly after the virtual photon interacts with the struck quark. When one integrates over the nearly-on-shell intermediate state, the amplitude acquires an imaginary part. Thus the rescattering of the quark produces a separated color-singlet $s\bar{s}$ and an imaginary phase. In the case of the light-cone gauge $A^+ = \eta \cdot A = 0$, one must also consider the final-state interactions of the (unstruck) \bar{s} quark. The gluon propagator in light-cone gauge $d_{LC}^{\mu\nu}(k) = (i/k^2 + i\epsilon)[-g^{\mu\nu} + (\eta^\mu k^\nu + k^\mu \eta^\nu / \eta \cdot k)]$ is singular at $k^+ = \eta \cdot k = 0$. The momentum of the exchanged gluon k^+ is of $\mathcal{O}(1/\nu)$; thus rescattering contributes at leading twist even in light-cone gauge. The net result is gauge invariant and is identical to the color dipole model calculation. The calculation of the rescattering effects on DIS in Feynman and light-cone gauge through three loops is given in detail for an Abelian model in the references [30]. The result shows that the rescattering corrections reduce the magnitude of the DIS cross section in analogy to nuclear shadowing.

A new understanding of the role of final-state interactions in deep inelastic scattering has thus emerged. The multiple scattering of the struck parton via instantaneous interactions in the target generates dominantly imaginary diffractive amplitudes, giving rise to an effective “hard pomeron” exchange. The presence of a rapidity gap between the target and diffractive system requires that the target remnant emerges in a color-singlet state; this is

made possible in any gauge by the soft rescattering. The resulting diffractive contributions leave the target intact and do not resolve its quark structure; thus there are contributions to the DIS structure functions which cannot be interpreted as parton probabilities [30]; the leading-twist contribution to DIS from rescattering of a quark in the target is a coherent effect which is not included in the light-front wave functions computed in isolation. One can augment the light-front wave functions with a gauge link corresponding to an external field created by the virtual photon $q\bar{q}$ pair current [23,21]. Such a gauge link is process dependent [24], so the resulting augmented LFWFs are not universal [23,30,31]. We also note that the shadowing of nuclear structure functions is due to the destructive interference between multi-nucleon amplitudes involving diffractive DIS and on-shell intermediate states with a complex phase. In contrast, the wave function of a stable target is strictly real since it does not have on-energy-shell intermediate state configurations. The physics of rescattering and shadowing is thus not included in the nuclear light-front wave functions, and a probabilistic interpretation of the nuclear DIS cross section is precluded.

Rikard Enberg, Paul Hoyer, Gunnar Ingelman and I [32] have shown that the quark structure function of the effective hard pomeron has the same form as the quark contribution of the gluon structure function. The hard pomeron is not an intrinsic part of the proton; rather it must be considered as a dynamical effect of the lepton-proton interaction. Our QCD-based picture also applies to diffraction in hadron-initiated processes. The rescattering is different in virtual photon- and hadron-induced processes due to the different color environment, which accounts for the observed non-universality of diffractive parton distributions. This framework also provides a theoretical basis for the phenomenologically successful Soft Color Interaction (SCI) model [33] which includes rescattering effects and thus generates a variety of final states with rapidity gaps.

The phase structure of hadron matrix elements is thus an essential feature of hadron dynamics. Although the LFWFs are real for a stable hadron, they acquire phases from initial state and final state interactions. In addition, the violation of CP invariance leads to a specific phase structure of the LFWFs. Dae Sung Hwang, Susan Gardner and I [34] have shown that this in turn leads to the electric dipole moment of the hadron and a general relation between the edm and anomalous magnetic moment Fock state by Fock state.

There are also leading-twist diffractive contributions $\gamma^* N_1 \rightarrow (q\bar{q})N_1$ arising from Reggeon exchanges in the t -channel [35]. For example, isospin-non-singlet $C = +$ Reggeons contribute to the difference of proton and neutron structure functions, giving the characteristic Kutiv Weisskopf $F_{2p} - F_{2n} \sim x^{1-\alpha_R(0)} \sim x^{0.5}$ behavior at small x . The x dependence of the structure functions reflects the Regge behavior $\nu^{\alpha_R(0)}$ of the virtual Compton amplitude at fixed Q^2 and $t = 0$. The phase of the diffractive amplitude is determined by analyticity and crossing to be proportional to $-1 + i$ for $\alpha_R = 0.5$, which together with the phase from the Glauber cut, leads to *constructive* in-

interference of the diffractive and nondiffractive multi-step nuclear amplitudes. Furthermore, because of its x dependence, the nuclear structure function is enhanced precisely in the domain $0.1 < x < 0.2$ where antishadowing is empirically observed. The strength of the Reggeon amplitudes is fixed by the fits to the nucleon structure functions, so there is little model dependence. Ivan Schmidt, Jian-Jun Yang, and I [36] have applied this analysis to the shadowing and antishadowing of all of the electroweak structure functions. Quarks of different flavors will couple to different Reggeons; this leads to the remarkable prediction that nuclear antishadowing is not universal; it depends on the quantum numbers of the struck quark. This picture leads to substantially different antishadowing for charged and neutral current reactions, thus affecting the extraction of the weak-mixing angle θ_W . We find that part of the anomalous NuTeV result [37] for θ_W could be due to the non-universality of nuclear antishadowing for charged and neutral currents. Detailed measurements of the nuclear dependence of individual quark structure functions are thus needed to establish the distinctive phenomenology of shadowing and antishadowing and to make the NuTeV results definitive. Antishadowing can also depend on the target and beam polarization.

3 The Conformal Approximation to QCD

One of the most interesting recent developments in hadron physics has been the use of Anti-de Sitter space holographic methods in order to obtain a first approximation to nonperturbative QCD. The essential principle underlying the AdS/CFT approach to conformal gauge theories is the isomorphism of the group of Poincaré and conformal transformations $SO(2,4)$ to the group of isometries of Anti-de Sitter space. The AdS metric is

$$ds^2 = \frac{R^2}{z^2} (\eta^{\mu\nu} dx_\mu dx_\nu - dz^2),$$

which is invariant under scale changes of the coordinate in the fifth dimension $z \rightarrow \lambda z$ and $dx_\mu \rightarrow \lambda dx_\mu$. Thus one can match scale transformations of the theory in 3+1 physical space-time to scale transformations in the fifth dimension z . The amplitude $\phi(z)$ represents the extension of the hadron into the fifth dimension. The behavior of $\phi(z) \rightarrow z^\Delta$ at $z \rightarrow 0$ must match the twist-dimension of the hadron at short distances $x^2 \rightarrow 0$. As shown by Polchinski and Strassler [38], one can simulate confinement by imposing the condition $\phi(z = z_0 = \frac{1}{\Lambda_{QCD}})$. This approach, has been successful in reproducing general properties of scattering processes of QCD bound states [38, 39], the low-lying hadron spectra [40, 41], hadron couplings and chiral symmetry breaking [41, 42], quark potentials in confining backgrounds [43] and pomeron physics [44].

It was originally believed that the AdS/CFT mathematical tool could only be applicable to strictly conformal theories such as $\mathcal{N} = 4$ supersymmetry. However, if one considers a semi-classical approximation to QCD with

massless quarks and without particle creation or absorption, then the resulting β function is zero, the coupling is constant, and the approximate theory is scale and conformal invariant. Conformal symmetry is of course broken in physical QCD; nevertheless, one can use conformal symmetry as a *template*, systematically correcting for its nonzero β function as well as higher-twist effects. For example, “commensurate scale relations” [45] which relate QCD observables to each other, such as the generalized Crewther relation [46], have no renormalization scale or scheme ambiguity and retain a convergent perturbative structure which reflects the underlying conformal symmetry of the classical theory. In general, the scale is set such that one has the correct analytic behavior at the heavy particle thresholds [47].

In a confining theory where gluons have an effective mass, all vacuum polarization corrections to the gluon self-energy decouple at long wavelength. Theoretical [48] and phenomenological [49] evidence is in fact accumulating that QCD couplings based on physical observables such as τ decay [50] become constant at small virtuality; *i.e.*, effective charges develop an infrared fixed point in contradiction to the usual assumption of singular growth in the infrared. The near-constant behavior of effective couplings also suggests that QCD can be approximated as a conformal theory even at relatively small momentum transfer. The importance of using an analytic effective charge [51] such as the pinch scheme [52, 53] for unifying the electroweak and strong couplings and forces is also important [54]. Thus conformal symmetry is a useful first approximant even for physical QCD.

4 Hadronic Spectra in AdS/QCD

Guy de Téramond and I [1, 40] have recently shown how a holographic model based on truncated AdS space can be used to obtain the hadronic spectrum of light quark $q\bar{q}$, qqq and gg bound states. Specific hadrons are identified by the correspondence of the amplitude in the fifth dimension with the twist-dimension of the interpolating operator for the hadron’s valence Fock state, including its orbital angular momentum excitations. An interesting aspect of our approach is to show that the mass parameter μR which appears in the string theory in the fifth dimension is quantized, and that it appears as a Casimir constant governing the orbital angular momentum of the hadronic constituents analogous to $L(L+1)$ in the radial Schrödinger equation.

As an example, the set of three-quark baryons with spin 1/2 and higher is described in AdS/CFT by the Dirac equation in the fifth dimension [1]

$$[z^2 \partial_z^2 - 3z \partial_z + z^2 \mathcal{M}^2 - \mathcal{L}_\pm^2 + 4] \psi_\pm(z) = 0. \quad (1)$$

The constants $\mathcal{L}_+ = L+1$, $\mathcal{L}_- = L+2$ in this equation are Casimir constants which are determined to match the twist dimension of the solutions with arbitrary relative orbital angular momentum. The solution is

$$\Psi(x, z) = C e^{-iP \cdot x} [\psi(z)_+ u_+(P) + \psi(z)_- u_-(P)], \quad (2)$$

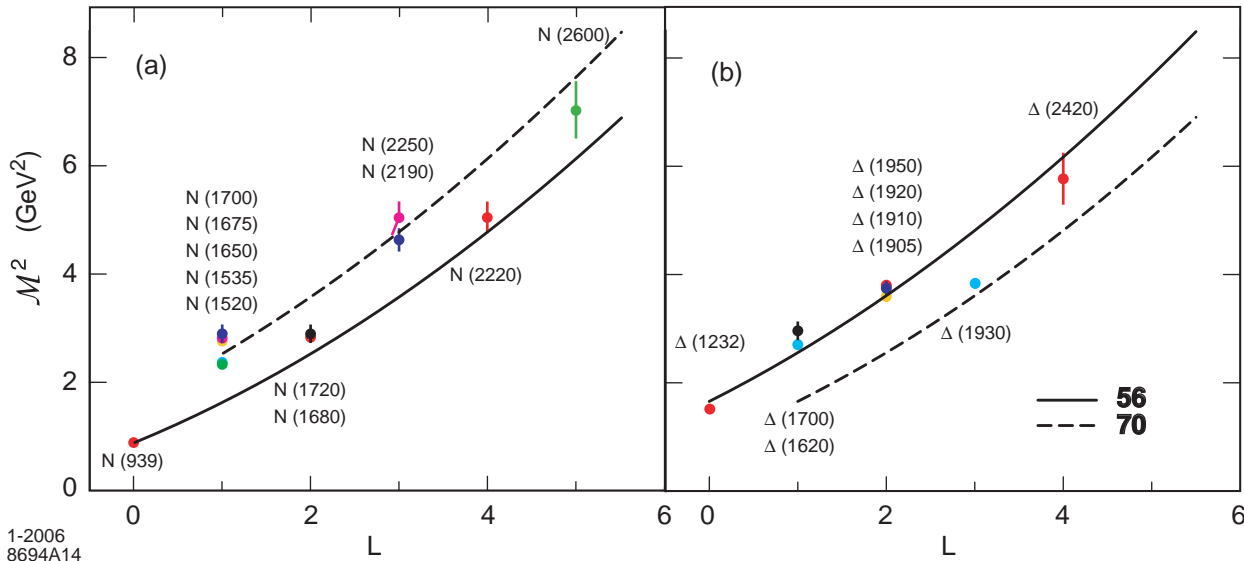


Fig. 2. Predictions for the light baryon orbital spectrum for $\Lambda_{QCD} = 0.25$ GeV. The **56** trajectory corresponds to L even $P = +$ states, and the **70** to L odd $P = -$ states.

with $\psi_+(z) = z^2 J_{1+L}(z\mathcal{M})$ and $\psi_-(z) = z^2 J_{2+L}(z\mathcal{M})$. The physical string solutions have plane waves and chiral spinors $u(P)_\pm$ along the Poincaré coordinates and hadronic invariant mass states given by $P_\mu P^\mu = \mathcal{M}^2$. A discrete four-dimensional spectrum follows when we impose the boundary condition $\psi_\pm(z = 1/\Lambda_{QCD}) = 0$. One has $\mathcal{M}_{\alpha,k}^+ = \beta_{\alpha,k} \Lambda_{QCD}$, $\mathcal{M}_{\alpha,k}^- = \beta_{\alpha+1,k} \Lambda_{QCD}$, with a scale-independent mass ratio [40]. The $\beta_{\alpha,k}$ are the first zeros of the Bessel eigenfunctions.

Figure 2(a) shows the predicted orbital spectrum of the nucleon states and Fig. 2(b) the Δ orbital resonances. The spin 3/2 trajectories are determined from the corresponding Rarita-Schwinger equation. The data for the baryon spectra are from S. Eidelman *et al.* [55]. The internal parity of states is determined from the SU(6) spin-flavor symmetry.

Since only one parameter, the QCD mass scale Λ_{QCD} , is introduced, the agreement with the pattern of physical states is remarkable. In particular, the ratio of Δ to nucleon trajectories is determined by the ratio of zeros of Bessel functions. The predicted mass spectrum in the truncated space model is linear $M \propto L$ at high orbital angular momentum, in contrast to the quadratic dependence $M^2 \propto L$ in the usual Regge parametrization.

Our approach shows that there is an exact correspondence between the fifth-dimensional coordinate of anti-de Sitter space z and a specific impact variable ζ in the light-front formalism which measures the separation of the constituents within the hadron in ordinary space-time. The amplitude $\Phi(z)$ describing the hadronic state in AdS₅ can be precisely mapped to the light-front wavefunctions $\psi_{n/h}$ of hadrons in physical space-time[1], thus providing a rel-

ativistic description of hadrons in QCD at the amplitude level. We derived this correspondence by noticing that the mapping of $z \rightarrow \zeta$ analytically transforms the expression for the form factors in AdS/CFT to the exact Drell-Yan-West expression in terms of light-front wavefunctions. In the case of a two-parton constituent bound state the correspondence between the string amplitude $\Phi(z)$ and the light-front wave function $\tilde{\psi}(x, \mathbf{b})$ is expressed in closed form [1]

$$\left| \tilde{\psi}(x, \zeta) \right|^2 = \frac{R^3}{2\pi} x(1-x) e^{3A(\zeta)} \frac{|\Phi(\zeta)|^2}{\zeta^4}, \quad (3)$$

where $\zeta^2 = x(1-x)\mathbf{b}_\perp^2$. Here b_\perp is the impact separation and Fourier conjugate to k_\perp . The variable ζ , $0 \leq \zeta \leq \Lambda_{QCD}^{-1}$, represents the invariant separation between point-like constituents, and it is also the holographic variable z in AdS; *i.e.*, we can identify $\zeta = z$. The prediction for the meson light-front wavefunction is shown in Fig. 3. We can also transform the equation of motion in the fifth dimension using the z to ζ mapping to obtain an effective two-particle light-front radial equation

$$\left[-\frac{d^2}{d\zeta^2} + V(\zeta) \right] \phi(\zeta) = \mathcal{M}^2 \phi(\zeta), \quad (4)$$

with the effective potential $V(\zeta) \rightarrow -(1-4L^2)/4\zeta^2$ in the conformal limit. The solution to (4) is $\phi(z) = z^{-\frac{3}{2}} \Phi(z) = Cz^{\frac{1}{2}} J_L(z\mathcal{M})$. This equation reproduces the AdS/CFT solutions. The lowest stable state is determined by the Breitenlohner-Freedman bound [56] and its eigenvalues by the boundary conditions at $\phi(z = 1/\Lambda_{QCD}) = 0$ and given

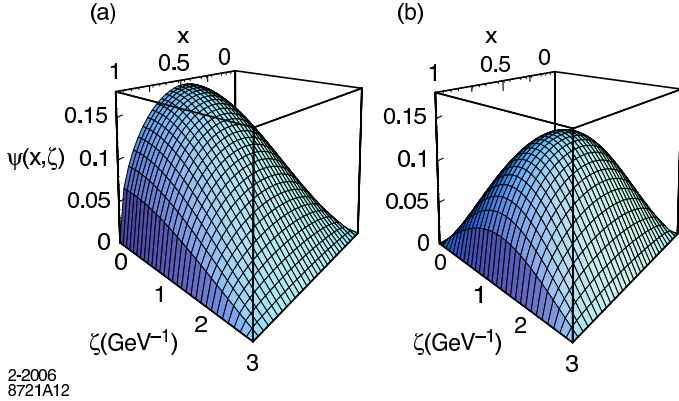


Fig. 3. AdS/QCD Predictions for the $L = 0$ and $L = 1$ LFWFs of a meson

in terms of the roots of the Bessel functions: $\mathcal{M}_{L,k} = \beta_{L,k} \Lambda_{\text{QCD}}$. Normalized LFWFs follow from (3)

$$\tilde{\psi}_{L,k}(x, \zeta) = B_{L,k} \sqrt{x(1-x)} J_L(\zeta \beta_{L,k} \Lambda_{\text{QCD}}) \theta(z \leq \Lambda_{\text{QCD}}^{-1}), \quad (5)$$

where $B_{L,k} = \pi^{-\frac{1}{2}} \Lambda_{\text{QCD}} J_{1+L}(\beta_{L,k})$. The resulting wavefunctions (see: Fig. 3) display confinement at large interquark separation and conformal symmetry at short distances, reproducing dimensional counting rules for hard exclusive processes in agreement with perturbative QCD.

The hadron form factors can be predicted from overlap integrals in AdS space or equivalently by using the Drell-Yan-West formula in physical space-time. The prediction for the pion form factor is shown in Fig. 4. The form factor at high Q^2 receives contributions from small ζ , corresponding to small $\mathbf{b}_\perp = \mathcal{O}(1/Q)$ (high relative $\mathbf{k}_\perp = \mathcal{O}(Q)$) as well as $x \rightarrow 1$. The AdS/CFT dynamics is thus distinct from endpoint models [57] in which the LFWF is evaluated solely at small transverse momentum or large impact separation.

The $x \rightarrow 1$ endpoint domain is often referred to as a "soft" Feynman contribution. In fact $x \rightarrow 1$ for the struck quark requires that all of the spectators have $x = k^+/P^+ = (k^0 + k^z)/P^+ \rightarrow 0$; this in turn requires high longitudinal momenta $k^z \rightarrow -\infty$ for all spectators – unless one has both massless spectator quarks $m \equiv 0$ with zero transverse momentum $k_\perp \equiv 0$, which is a regime of measure zero. If one uses a covariant formalism, such as the Bethe-Salpeter theory, then the virtuality of the struck quark becomes infinitely spacelike: $k_F^2 \sim -\frac{k_\perp^2 + m^2}{1-x}$ in the endpoint domain. Thus, actually, $x \rightarrow 1$ corresponds to high relative longitudinal momentum; it is as hard a domain in the hadron wavefunction as high transverse momentum.

It is also interesting to note that the distribution amplitude predicted by AdS/CFT at the hadronic scale is $\phi_\pi(x, Q) = \frac{4}{\sqrt{3}\pi} f_\pi \sqrt{x(1-x)}$ from both the harmonic oscillator and truncated space models is quite different than the asymptotic distribution amplitude predicted from the PQCD evolution [6] of the pion distribution amplitude $\phi_\pi(x, Q \rightarrow \infty) = \sqrt{3} f_\pi x(1-x)$. The broader shape of the pion distribution increases the magnitude of the leading

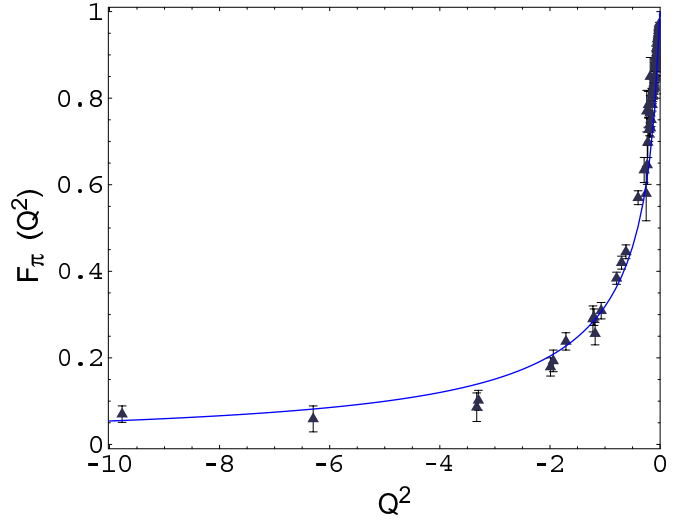


Fig. 4. AdS/QCD Predictions for the pion form factor.

twist perturbative QCD prediction for the pion form factor by a factor of 16/9 compared to the prediction based on the asymptotic form, bringing the PQCD prediction close to the empirical pion form factor [58].

Since they are complete and orthonormal, the AdS/CFT model wavefunctions can be used as an initial ansatz for a variational treatment or as a basis for the diagonalization of the light-front QCD Hamiltonian. We are now in fact investigating this possibility with J. Vary and A. Harindranath. The wavefunctions predicted by AdS/QCD have many phenomenological applications ranging from exclusive B and D decays, deeply virtual Compton scattering and exclusive reactions such as form factors, two-photon processes, and two body scattering. A connection between the theories and tools used in string theory and the fundamental constituents of matter, quarks and gluons, has thus been found.

The application of AdS/CFT to QCD phenomenology is now being developed in many new directions, incorporating finite quark masses, chiral symmetry breaking, asymptotic freedom, and finite temperature effects. Some recent papers are given in refs. [59–68].

Acknowledgments

Work supported by the Department of Energy under contract number DE-AC02-76SF00515. The AdS/CFT results reported here were done in collaboration with Guy de Téramond.

References

1. S. J. Brodsky and G. F. de Téramond, Phys. Rev. Lett. **96**, 201601 (2006) [arXiv:hep-ph/0602252].

2. P. A. M. Dirac, *Rev. Mod. Phys.* **21**,392(1949).
3. S. J. Brodsky, H. C. Pauli and S. S. Pinsky, *Phys. Rept.* **301**, 299 (1998) [arXiv:hep-ph/9705477].
4. S. J. Brodsky and D. S. Hwang, *Nucl. Phys. B* **543**, 239 (1999) [arXiv:hep-ph/9806358].
5. S. J. Brodsky, M. Diehl and D. S. Hwang, *Nucl. Phys. B* **596**, 99 (2001) [arXiv:hep-ph/0009254].
6. G. P. Lepage and S. J. Brodsky, *Phys. Lett. B* **87**,359(1979).
7. A. V. Efremov and A. V. Radyushkin, *Phys. Lett. B* **94**, 245 (1980).
8. G. P. Lepage and S. J. Brodsky, *Phys. Rev. D* **22**, 2157 (1980).
9. S. J. Brodsky and G. P. Lepage, SLAC-PUB-2294. *Presented at Workshop on Current Topics in High Energy Physics, Cal Tech., Pasadena, Calif., Feb 13-17, 1979.*
10. S. J. Brodsky, arXiv:hep-ph/0004211.
11. S. J. Brodsky, C. R. Ji and G. P. Lepage, *Phys. Rev. Lett.* **51**, 83 (1983).
12. S. J. Brodsky, D. S. Hwang and I. Schmidt, *Phys. Lett. B* **530**, 99 (2002) [arXiv:hep-ph/0201296].
13. M. Burkardt, *Nucl. Phys. Proc. Suppl.* **141**, 86 (2005) [arXiv:hep-ph/0408009].
14. A. Airapetian *et al.* [HERMES Collaboration], *Phys. Rev. Lett.* **94**, 012002 (2005) [arXiv:hep-ex/0408013].
15. H. Avakian and L. Elouadrhiri [CLAS Collaboration], *AIP Conf. Proc.* **698**, 612 (2004).
16. M. Burkardt, *Int. J. Mod. Phys. A* **21**, 926 (2006) [arXiv:hep-ph/0509316].
17. X. d. Ji, *Phys. Rev. Lett.* **91**, 062001 (2003) [arXiv:hep-ph/0304037].
18. S. J. Brodsky, D. Chakrabarti, A. Harindranath, A. Mukherjee and J. P. Vary, arXiv:hep-ph/0604262.
19. P. Hoyer, arXiv:hep-ph/0608295.
20. S. J. Brodsky and S. Gardner, arXiv:hep-ph/0608219.
21. J. C. Collins and A. Metz, *Phys. Rev. Lett.* **93**, 252001 (2004) [arXiv:hep-ph/0408249].
22. X. d. Ji and F. Yuan, *Phys. Lett. B* **543**, 66 (2002) [arXiv:hep-ph/0206057].
23. A. V. Belitsky, X. Ji and F. Yuan, *Nucl. Phys. B* **656**, 165 (2003) [arXiv:hep-ph/0208038].
24. J. C. Collins, *Phys. Lett. B* **536**, 43 (2002) [arXiv:hep-ph/0204004].
25. S. J. Brodsky, D. S. Hwang and I. Schmidt, *Nucl. Phys. B* **642**, 344 (2002) [arXiv:hep-ph/0206259].
26. D. Boer, S. J. Brodsky and D. S. Hwang, *Phys. Rev. D* **67**, 054003 (2003) [arXiv:hep-ph/0211110].
27. C. Adloff *et al.* [H1 Collaboration], *Z. Phys. C* **76**, 613 (1997) [arXiv:hep-ex/9708016].
28. J. Breitweg *et al.* [ZEUS Collaboration], *Eur. Phys. J. C* **6**, 43 (1999) [arXiv:hep-ex/9807010].
29. S. J. Brodsky, L. Frankfurt, J. F. Gunion, A. H. Mueller and M. Strikman, *Phys. Rev. D* **50**, 3134 (1994) [arXiv:hep-ph/9402283].
30. S. J. Brodsky, P. Hoyer, N. Marchal, S. Peigne and F. Sannino, *Phys. Rev. D* **65**, 114025 (2002) [arXiv:hep-ph/0104291].
31. J. C. Collins, *Acta Phys. Polon. B* **34**, 3103 (2003) [arXiv:hep-ph/0304122].
32. S. J. Brodsky, R. Enberg, P. Hoyer and G. Ingelman, *Phys. Rev. D* **71**, 074020 (2005) [arXiv:hep-ph/0409119].
33. A. Edin, G. Ingelman and J. Rathsman, *Phys. Lett. B* **366**, 371 (1996) [arXiv:hep-ph/9508386].
34. S. J. Brodsky, S. Gardner and D. S. Hwang, *Phys. Rev. D* **73**, 036007 (2006) [arXiv:hep-ph/0601037].
35. S. J. Brodsky and H. J. Lu, *Phys. Rev. Lett.* **64**, 1342 (1990).
36. S. J. Brodsky, I. Schmidt and J. J. Yang, *Phys. Rev. D* **70**, 116003 (2004) [arXiv:hep-ph/0409279].
37. G. P. Zeller *et al.* [NuTeV Collaboration], *Phys. Rev. Lett.* **88**, 091802 (2002) [Erratum-ibid. **90**, 239902 (2003)] [arXiv:hep-ex/0110059].
38. J. Polchinski and M. J. Strassler, *Phys. Rev. Lett.* **88**, 031601 (2002) [arXiv:hep-th/0109174].
39. S. J. Brodsky and G. F. de Teramond, *Phys. Lett. B* **582**, 211 (2004) [arXiv:hep-th/0310227].
40. G. F. de Teramond and S. J. Brodsky, *Phys. Rev. Lett.* **94**, 201601 (2005) [arXiv:hep-th/0501022].
41. J. Erlich, E. Katz, D. T. Son and M. A. Stephanov, *Phys. Rev. Lett.* **95**, 261602 (2005) [arXiv:hep-ph/0501128].
42. S. Hong, S. Yoon and M. J. Strassler, arXiv:hep-ph/0501197.
43. H. Boschi-Filho, N. R. F. Braga and C. N. Ferreira, *Phys. Rev. D* **73**, 106006 (2006) [arXiv:hep-th/0512295].
44. R. C. Brower, J. Polchinski, M. J. Strassler and C. I. Tan, [arXiv:hep-th/0603115].
45. S. J. Brodsky and H. J. Lu, *Phys. Rev. D* **51**, 3652 (1995) [arXiv:hep-ph/9405218].
46. S. J. Brodsky, G. T. Gabadadze, A. L. Kataev and H. J. Lu, *Phys. Lett. B* **372**, 133 (1996) [arXiv:hep-ph/9512367].
47. S. J. Brodsky, G. P. Lepage and P. B. Mackenzie, *Phys. Rev. D* **28**, 228 (1983).
48. R. Alkofer, C. S. Fischer and F. J. Llanes-Estrada, *Phys. Lett. B* **611**, 279 (2005) [arXiv:hep-th/0412330].
49. S. J. Brodsky, S. Menke, C. Merino and J. Rathsman, *Phys. Rev. D* **67**, 055008 (2003) [arXiv:hep-ph/0212078].
50. S. J. Brodsky, J. R. Pelaez and N. Toumbas, *Phys. Rev. D* **60**, 037501 (1999) [arXiv:hep-ph/9810424].
51. S. J. Brodsky, M. S. Gill, M. Melles and J. Rathsman, *Phys. Rev. D* **58**, 116006 (1998) [arXiv:hep-ph/9801330].
52. M. Binger and S. J. Brodsky, arXiv:hep-ph/0602199.
53. J. M. Cornwall and J. Papavassiliou, *Phys. Rev. D* **40**, 3474 (1989).
54. M. Binger and S. J. Brodsky, *Phys. Rev. D* **69**, 095007 (2004) [arXiv:hep-ph/0310322].
55. S. Eidelman *et al.* [Particle Data Group], *Phys. Lett. B* **592**, 1 (2004).
56. P. Breitenlohner and D. Z. Freedman, *Annals Phys.* **144**, 249 (1982).
57. A. V. Radyushkin, arXiv:hep-ph/0605116.
58. H. M. Choi and C. R. Ji, arXiv:hep-ph/0608148.
59. N. Evans and A. Tedder, arXiv:hep-ph/0609112.
60. Y. Kim, S. J. Sin, K. H. Jo and H. K. Lee, arXiv:hep-ph/0609008.
61. C. Csaki and M. Reece, arXiv:hep-ph/0608266.
62. J. Erdmenger, N. Evans and J. Grosse, arXiv:hep-th/0605241.
63. H. Boschi-Filho and N. R. F. Braga, arXiv:hep-th/0604091.
64. N. Evans and T. Waterson, arXiv:hep-ph/0603249.
65. M. Harada, S. Matsuzaki and K. Yamawaki, arXiv:hep-ph/0603248.
66. G. T. Horowitz and J. Polchinski, arXiv:gr-qc/0602037.
67. I. R. Klebanov, *Int. J. Mod. Phys. A* **21**, 1831 (2006) [arXiv:hep-ph/0509087].
68. E. Shuryak, arXiv:hep-th/0605219.